# Structural Settings of Convective Hydrothermal Systems in Southeastern British Columbia (Parts of NTS 082E–G, J–O, 083C, D)

**T.D. Finley**[1], **Department of Earth and Atmospheric Sciences, University of Alberta, Edmonton, Alberta, tfinley@ualberta.ca**

**S.T. Johnston, Department of Earth and Atmospheric Sciences, University of Alberta, Edmonton, Alberta**

**M.J. Unsworth, Department of Physics, University of Alberta, Edmonton, Alberta**

**J. Banks, Department of Earth and Atmospheric Sciences, University of Alberta, Edmonton, Alberta**

**D. Pana, Alberta Energy Regulator / Alberta Geological Survey, Edmonton, Alberta**

**C. Hanneson, Department of Physics, University of Alberta, Edmonton, Alberta**

Finley, T.D., Johnston, S.T., Unsworth, M.J., Banks, J., Pana, D. and Hanneson, C. (2020): Structural settings of convective hydrothermal systems in southeastern British Columbia (parts of NTS 082E–G, J–O, 083C, D); *in* Geoscience BC Summary of Activities 2019: Energy and Water, Geoscience BC, Report 2020-02, p. 115–130.

## Introduction

There has long been interest in developing geothermal energy in western Canada (Jessop et al., 1991; Grasby et al., 2012), but as yet, there are no operating geothermal power plants or direct heating systems (excluding shallow geo-exchange). Part of the problem is limited geological understanding of the regions where geothermal potential is highest, particularly the complexly deformed Canadian Cordillera of British Columbia (BC) and Yukon. Crustal heat flow in the Cordillera is relatively high (~80–100 milliwatts per square metre [mW/m$^2$]; Davis and Lewis, 1984), and the occurrence of more than 130 thermal springs has attracted the interest of geothermal developers. However, data constraining the subsurface are limited, which discourages investment.

Most geothermal systems occur in magmatically and tectonically active areas (e.g., western United States, Japan, New Zealand, Iceland). This is due in part to the elevated enthalpy in the crust, but also to the enhanced permeability of brittle faults, which act as conduits for circulating hydrothermal fluids (Moeck, 2014). Several characteristics of fault zones influence their structure, including age and amount of seismic activity (e.g., Curewitz and Karson, 1997), kinematics (e.g., Meixner et al., 2016) and subsurface geometry (e.g., Moreno et al., 2018). Understanding these parameters is key to understanding the geothermal systems fault zones may host.

Hydrothermal systems (i.e., thermal springs) in the Canadian Cordillera are broadly associated with major fault zones (Grasby and Hutcheon, 2001). However, detailed investigations of the significant hydrogeological properties of many of these faults have not previously been conducted. The research presented in this paper focuses on hydrothermal systems in three specific regions in the southern Canadian Cordillera (Figure 1b): Valemount and Canoe Reach, Nakusp and the West Kootenays, and the southern Rocky Mountain Trench. These regions were chosen because of their concentrations of high-temperature thermal springs, elevated crustal heat flow, proximity to population centres, and commercial interest in geothermal development in these areas. Herein are presented new structural data collected within fault zones that appear to control hydrothermal systems in these areas. The current stress field of the crust, and its relationship to fault kinematics and geometry is also considered. These data provide new insight into the age, kinematics and geometry of these fault zones.

## Background

### Regional Geology

The Canadian Cordillera is an ~800 km wide mountain belt that stretches from the Arctic Ocean to the United States border, mostly within the Northwest and Yukon territories and the provinces of British Columbia and Alberta. Its elevated topography, rugged relief and complex geology reflect a protracted and ongoing interaction between various oceanic plates, accreted terranes, and continental North America (Gabrielse and Yorath, 1991). For simplicity, the Cordillera is divided into five major morphogeological belts (Figure 1a; Gabrielse et al., 1991). The easternmost Foreland Belt is composed of folded and thrusted—but largely unmetamorphosed—carbonate and siliciclastic

[1]*The lead author is a 2019 Geoscience BC Scholarship recipient.*

*This publication is also available, free of charge, as colour digital files in Adobe Acrobat® PDF format from the Geoscience BC website: http://www.geosciencebc.com/updates/summary-of-activities/.*

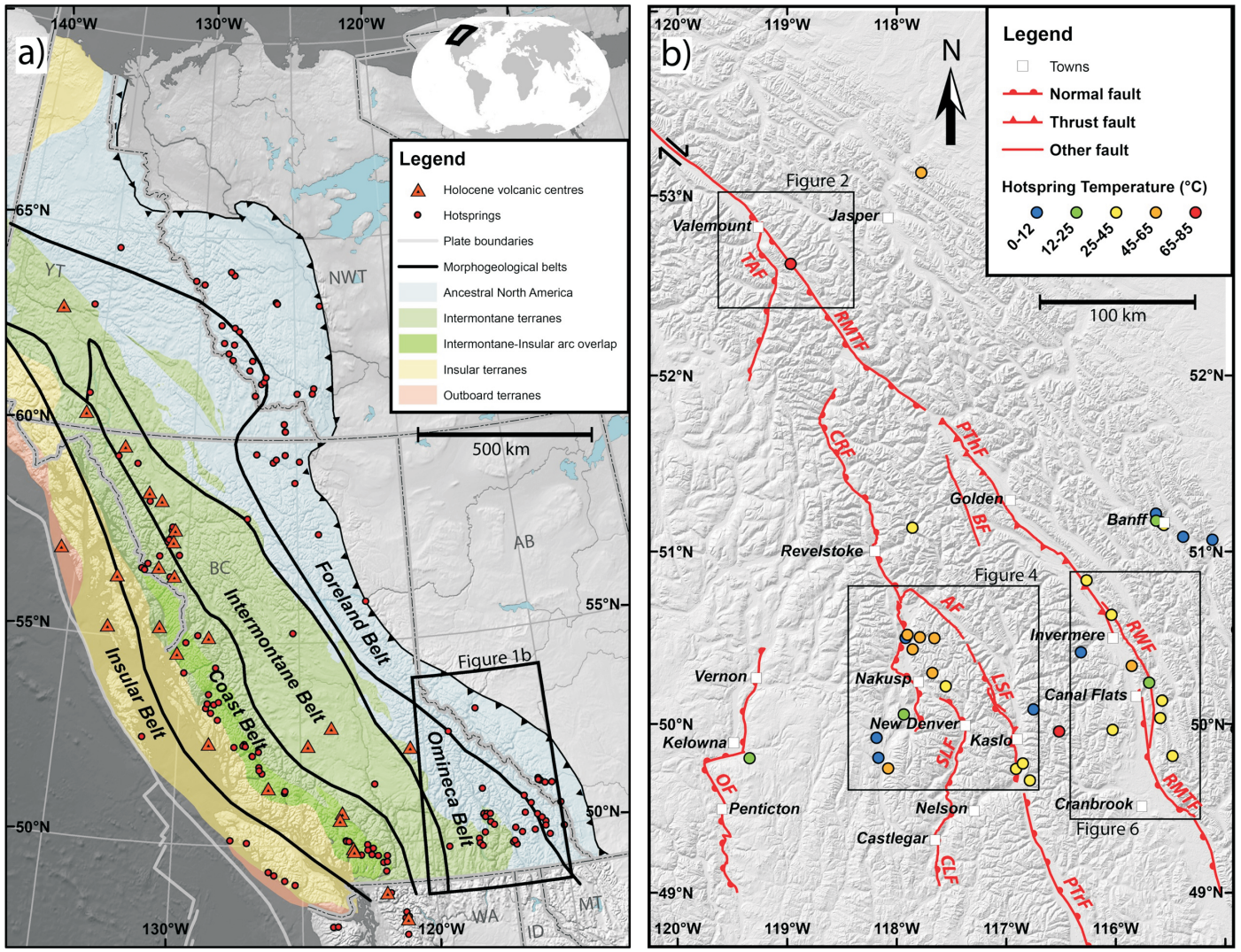


**Figure 1. a)** Regional geological setting of the Canadian Cordillera. Morphogeological belts are after Gabrielse et al. (1991), and the boundaries of allochthonous and autochthonous superterranes are after Colpron and Nelson (2011). Volcanoes active in the Holocene (American Geological Institute, 2003) occur predominantly within the Coast Belt. Concentrations of thermal springs occur along the axis of the Coast Belt, in the northern Omineca and Foreland belts, and in the southern Omineca and Foreland belts (Woodsworth and Woodsworth, 2014). Note that the latter two clusters do not correspond to regions of active volcanism, but do correspond to significant (>100 milliwatts per square metre [$mW/m^2$]) heat-flow anomalies (see Majorowicz and Grasby, 2010). The current study areas are located in the southern Omineca and Foreland belts. **b)** Major faults in southeastern British Columbia. Abbreviations: AF, Adit fault; BF, Beaver fault; CLF, Champion Lakes fault; CRF, Columbia River fault; LSF, Lakeshore fault; OF, Okanagan fault; PThF, Purcell Thrust fault; PTrF, Purcell Trench fault; RMTF, Rocky Mountain Trench fault; RWF, Redwall fault; SLF, Slocan Lake fault; TAF, Tintina fault.

rocks of an ancestral passive margin and a subsequent foreland basin. Adjacent and to the west is the Omineca Belt, which is dominantly composed of metamorphosed sedimentary rocks coeval with those in the Foreland Belt and deformed during the same mountain-building events. The Omineca Belt is intruded by numerous Jurassic and Cretaceous continental arc–type plutonic suites (Armstrong, 1988), and tectonic windows expose metamorphosed crystalline rocks, interpreted as cratonic basement exhumed during Eocene extension (Parrish et al., 1988). Contractional deformation of the Omineca and Foreland belts is associated with Jurassic and younger accretionary and collisional events, including accretion of oceanic arc terranes that make up the more westerly Intermontane Belt (Evenchick et al., 2007). West of the Intermontane Belt lies the Coast Belt, which is largely composed of intrusive and metamorphic rocks associated with the Cretaceous to Eocene subduction and accretion of the westernmost Insular Belt, which underlies Vancouver Island, Haida Gwaii and the Alaska Panhandle (Evenchick et al., 2007). Young and active continental arc volcanoes are being constructed atop the Coast Belt as a result of ongoing subduction of the Juan de Fuca Plate and other micro-plates off the western margin of the continent (Green et al., 1988). This study is focused on hydrothermal systems in the southern Omineca Belt, from the United States border to ~53°N (Figure 1b).

## Sources and Expressions of Heat Flow in the Canadian Cordillera

The Cordillera is one of the most promising regions in Canada for geothermal energy development due to its high heat flow and steep geothermal gradients (Grasby et al., 2012). Whereas much of eastern and central Canada is underlain by old and cold cratonic lithosphere and ancient orogenic belts, the Cordillera is geologically young and is subject to ongoing tectonic and magmatic processes that enhance geothermal conditions. The presence of more than 130 thermal springs throughout the Cordillera (Figure 1a) provides a first-order indication that heat flow might be sufficient for geothermal energy extraction. Outlet temperatures of these springs range from ~20° to 80°C (Woodsworth and Woodsworth, 2014). Aqueous geothermometry indicates that the maximum temperatures reached by some of these systems exceeds 180°C, with maximum circulation depths estimated to be ~2–5 km (Grasby and Hutcheon, 2001; Allen et al., 2006; Caron et al., 2007). Although thermal springs are not necessarily the best indicator of geothermal prospectivity (Ferguson and Grasby, 2011), they do provide a basic indication of geothermal resource potential, in a subsurface environment that is otherwise poorly constrained by data.

The geothermal gradient of the Cordillera ranges from ~20° to 50°C/km (Hitchon, 1984; Lewis et al., 1992; Grasby and Hutcheon, 2001). These values, though lower than most conventional (high enthalpy) geothermal energy resources, are similar to gradients measured in low enthalpy systems being explored and developed for electricity generation in Europe and New Zealand (e.g., Agemar et al., 2014; Reyes, 2015; Farquharson et al., 2016). Crustal heat flow in the Cordillera ranges from ~40 to 130 mW/m$^2$ (Hyndman and Lewis, 1995; Blackwell and Richards, 2004; Majorowicz and Grasby, 2010). Heat flow is locally very high (>200 mW/m$^2$) near active volcanoes in the Garibaldi volcanic belt in southwestern BC (e.g., Mount Meager), but these values do not reflect the bulk of thermal conditions in the Cordillera. In several broad regions heat flow exceeds 100 mW/m$^2$ (see Majorowicz and Grasby, 2010), which is comparable to geothermal energy–producing regions like Nevada and Utah (Blackwell and Richards, 2004). Interestingly, one of these regions, the southern Omineca Belt (Columbia Mountains) of southeastern BC, does not contain any active or recently active volcanoes, which suggests that the heat might come from shallow intrusions in the crust. Indeed, radioactive heat generation measured in Cretaceous and Paleogene intrusive suites is high in the Omineca Belt (Lewis et al., 1992).

## Major Fault Zones and their Relation to Hydrothermal Systems

Grasby and Hutcheon (2001) compared several parameters, including heat flow, permeability, topography/relief, infiltration rate, and the presence of fault zones, with regards to their influence on the location of thermal springs in the southern Canadian Cordillera. Ultimately they determined that—with the exception of springs within the Garibaldi volcanic belt—fault zones act as a primary control on the position of thermal springs in the Canadian Cordillera, whereas the other factors have a negligible influence. From east to west, the significant fault zones in the southeastern Cordillera identified by Grasby and Hutcheon (2001) as hydrogeologically significant are (see Figure 1b): the southern Rocky Mountain Trench fault (RMTF), Purcell Trench fault (PTrF), Columbia River fault (CRF), and Okanagan fault (OF). All of these structures have been interpreted as hosting significant normal displacement during Eocene extension of the Cordillera (Parrish et al., 1988; van der Velden and Cook, 1996).

Fault zones typically have an anisotropic permeability structure, dependent on the relative percentages of clay fault gouge and fractured wall rock (Caine et al., 1996). Typically, cross-fault flow is impeded by the impermeable (clay rich) core material, while along-fault flow is facilitated by the permeable damaged (fractured) zone. Grasby and Hutcheon (2001) presented a conceptual model for hydrothermal convection cells in the Canadian Cordillera in which meteoric water percolates vertically down through the crust until it encounters a shallowly dipping fault plane, and is then forced back up to the surface via the damaged

zone conduit. Because faults tend to crop out in valleys due to accelerated erosion of comminuted fault rock, there is a natural topographic drive to such systems, with recharge occurring in mountainous highlands.

What remains unanswered is why certain faults host thermal springs while others do not, and why thermal springs are distributed unevenly along fault zones. Variations in crustal heat flow, precipitation/infiltration rate, and topographic relief occur on wavelengths too broad to explain the pattern of hotspring occurrence (Grasby and Hutcheon, 2001; Ferguson and Grasby, 2011). It is therefore likely that inter- and intra-fault variations in geometry and permeability structure are critical parameters. It has been shown in other structurally controlled geothermal systems that the current stress state of the crust and resulting fault kinematics can predict which fault segments are most permeable; faults oriented parallel or oblique to $S_{Hmax}$ (maximum horizontal compression) are more likely to be permeable than those oriented perpendicular to $S_{Hmax}$ (e.g., Meixner et al., 2016). Furthermore, there is a positive relationship between strain rate and fault permeability—seismic activity has been shown to maintain fault permeability via episodic refracturing of minerals precipitating within the fault zone (Curewitz and Karson, 1997). Below, these parameters are discussed for major faults in three areas of southeastern BC (Figure 1b).

## Structural Settings of Hydrothermal Systems in the Canadian Cordillera

### Valemount and Canoe Reach

#### Background

The town of Valemount has attracted commercial interest in geothermal energy production due to the presence of the Canoe River thermal spring ~30 km south of the townsite, on the west shore of Kinbasket Lake hydroelectric reservoir (Figure 2) in the southern Rocky Mountain Trench (SRMT). The Canoe River spring is one of the hottest thermal springs in BC, with outlet temperatures measured at 80°C and maximum temperatures derived from aqueous geothermometers exceeding 200°C (Ghomshei, 2007). The Town of Valemount is interested in the possibility of low-carbon baseload power and heat, along with the tourism draw that a geothermal spa would bring. Recently, Borealis GeoPower has undertaken a geothermal exploration program in the area, conducting soil sampling, geophysical surveying and slim-hole drilling (see http://www.borealisgeopower.com/).

The crustal structure of the Valemount area is complex (Figure 2), and there are limited constraints on the structures that might control hydrothermal circulation. Much of the area is underlain by Paleoproterozoic basement gneiss, referred to as the Malton Gneiss on the southwest side of the SRMT valley, and the Bulldog and Yellowjacket gneisses on the northeast side. Some authors have asserted that the eastern and western gneiss packages are geochemically and geophysically distinct, arguing for a major transcurrent fault between them (Chamberlain and Lambert, 1985; Chamberlain et al., 1985). However, all three packages are similar, and may represent exhumed cratonic basement (McDonough and Simony, 1988). The gneiss complex is overlain by a metasedimentary cover sequence assigned to the Neoproterozoic Miette Group. The gneiss complex and a thin slice of lower Miette Group are carried northeastward over middle and upper Miette rocks on the Bear Foot thrust, a synmetamorphic dextral-oblique reverse fault assumed to have accommodated 50 km of dip-slip displacement (McDonough and Simony, 1988, 1989). Orogen-parallel ductile stretching lineations in the footwall of the Bear Foot thrust indicate that the thrust predates Cenozoic brittle structures (McDonough and Simony, 1989). The Malton and Bulldog gneiss packages are carried in the hangingwall of the northeast-verging Purcell Thrust, a large, out-of-sequence thrust fault that is mapped for several hundred kilometres to the south (Price, 1981). The western extent of the Malton Gneiss is defined by the steeply west-dipping Thompson–Albreda fault, a fault associated with Eocene extension of the orogenic belt. Separating the Malton and Bulldog/Yellowjacket gneiss packages, on the floor of the SRMT, is the Rocky Mountain Trench fault, a steeply dipping west-side-down normal fault. Its exact trace is obscured by Quaternary cover and the hydroelectric reservoir, and its presence is inferred from offset metamorphic isograds and stratigraphic horizons. The RMT fault is mapped as far south as 52°N, where it disappears, and the trench floor is instead occupied by the Purcell Thrust fault. The RMT fault reappears south of Canal Flats and can be traced as far south as Flathead Lake in Montana. Notably, north of Valemount, the RMT fault and its northern continuation, the Tintina fault, are known to host significant dextral slip (Roddick, 1967; Gabrielse, 1985; McMechan, 2000). Murphy (1990) identified dextral mylonitic fabrics at the north end of Kinbasket Lake (12 km southeast of Valemount), but dextral strike-slip is not believed to continue any farther southeast along the SRMT, and transpression is instead accommodated on structures like the Fraser River fault ~250 km to the west (Price and Carmichael, 1986; Struik, 1993).

#### New Observations

Detailed structural fieldwork was conducted in the spring of 2018 in the Valemount area and south along Kinbasket Lake (Figures 2, 3). Work was focused on the shorelines of the reservoir in an attempt to capture kinematic indicators proximal to the RMT fault zone, which parallels the lakeshore. Nearly 150 measurements of fault plane and slickenline orientations were collected, especially in the continuous exposures of the basal Windermere Supergroup and

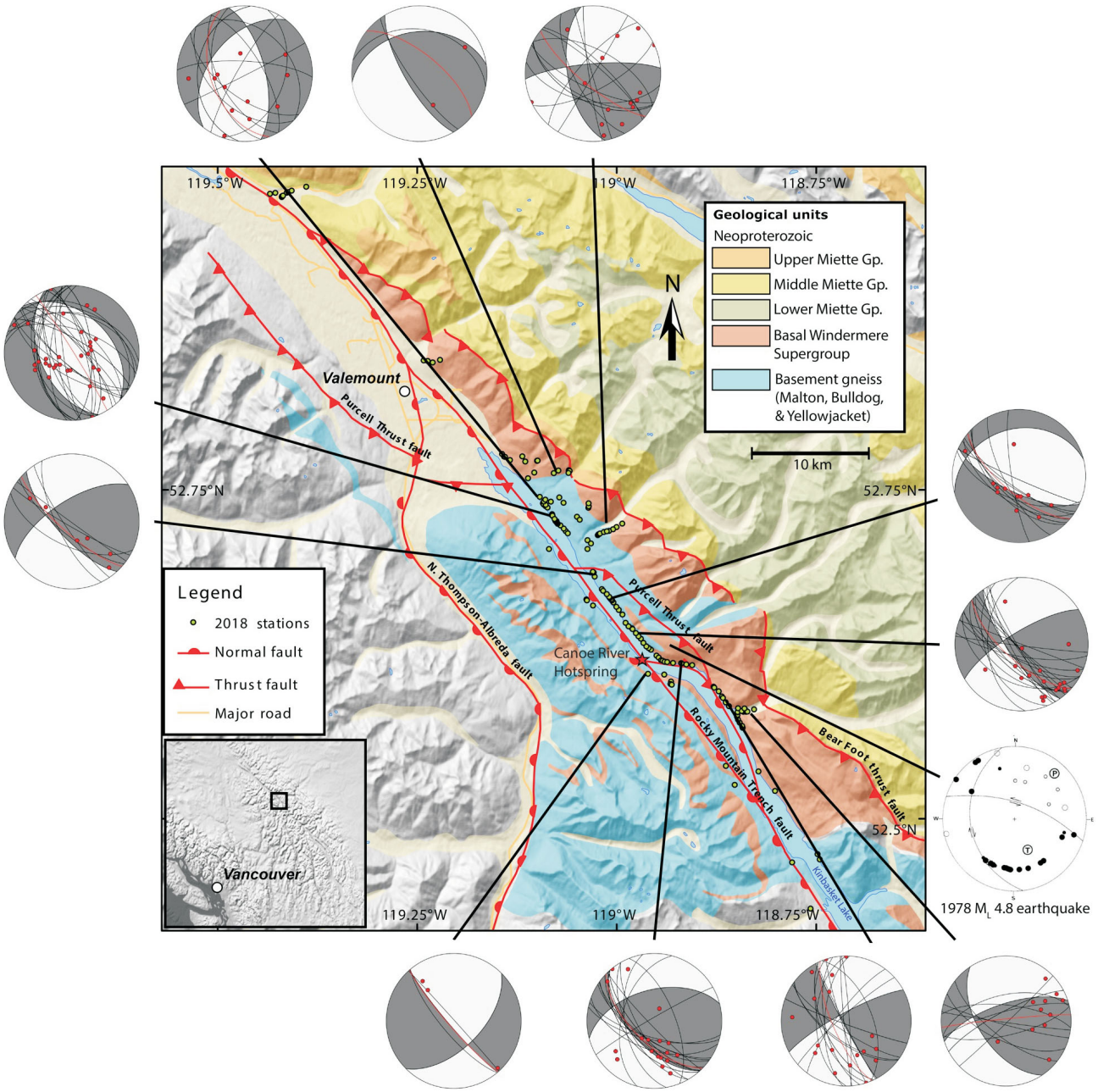


**Figure 2.** Geology of the Valemount and Canoe Reach area, on northern Kinbasket hydroelectric reservoir, south of Valemount, after Murphy (2007). Green dots are sites examined in the field. Lower-hemisphere stereonets ('beachball' plots) show fault plane and slickenline orientations for subsets of stations along Kinbasket Lake. Compressional (P) and dilational (T) quadrants represent the average kinematics for each subset. The focal mechanism for the 1978 Richter (local) magnitude ($M_L$) 4.8 McNaughton Lake earthquake (Rogers et al., 1980) is provided for comparison (lower right). Abbreviation: Gp., Group.

Bulldog Gneiss on the northeast side of the reservoir (Figure 3). Slickenlines were ranked according to confidence, and care was taken to avoid mistaking riedel shears for the more diagnostic mineral growths on the lee side of fault plane asperities. Abundant subhorizontal slickenlines were found, generally on subvertical fault planes on numerous outcrops, distributed for 40 km south along the lake. The majority of slickenlines indicated dextral slip. Few west-side-down dip-slip slickenlines were observed. Subsets of slickenlines were identified manually, and kinematic analysis was performed on each subset using the Orient software package (Vollmer, 2019). 'Beachball' plots (Figure 2) showing compressional (P) and dilational (T) quadrants were calculated based on the average kinematics of all faults within each subset.

A Richter (local) magnitude ($M_L$) 4.8 earthquake occurred in the area on May 14, 1978 (Rogers et al., 1980), and was initially investigated due to concerns that it may have been


**Figure 3. a)** View south from the north end of the Kinbasket hydroelectric reservoir, captured at low water level in May 2018. Red dot shows the location of the Canoe River thermal spring. **b)** Vestiges of dextral slickenlines in basal Neoproterozoic Windermere Supergroup on the northeast side of the lake (lat. 52.5691°N, long. 118.8420°W). Fault is oriented 168°/63°, slickenlines (red arrow) are oriented 19°→192°. **c)** Large, oxidized, fault plane in basal Windermere Supergroup on northeast side of lake (lat. 52.6202°N, long. 118.9424°W). Fault is oriented 170°/54°, dextral slickenlines (not pictured) are oriented 15°→333°. **d)** Dextral slickenlines in Paleoproterozoic Bulldog Gneiss on northeast side of lake (lat. 52.6412°N, long. 118.9759°W). Fault is oriented 139°/84°, slickenlines (red arrow) are oriented 15°→143°.

caused by the filling of the Kinbasket Lake reservoir (historically referred to as McNaughton Lake). The preferred focal mechanism for this earthquake was dominantly right lateral, with a reverse component, on a south-southeast–striking fault plane. Ultimately it was concluded that the earthquake was not induced by the reservoir, but rather was attributed to "stresses associated with residual strain energy stored during the mountain building process" (Rogers et al., 1980). The orientation of the focal mechanism of the McNaughton Lake earthquake is similar to the orientation of fault planes and slickenlines observed in the area (Figure 2).

## Nakusp and the West Kootenay Region

### Background

The West Kootenay region of southeastern BC has some of the highest heat flow values in Canada (Blackwell and Richards, 2004; Majorowicz and Grasby, 2010), and the town of Nakusp bills itself as the Hot Spring capital of Canada. Some of Canada's hottest thermal springs, with the highest estimates of maximum temperatures (Grasby and Hutcheon, 2001), exist in the area. Many thermal springs in this area issue from the Kuskanax batholith (Figure 4), a mid-Jurassic (173 ±5 Ma) batholith that underlies most of the mountain range to the northeast of Nakusp (Parrish and Wheeler, 1983).

There are two fault zones in this area that are likely significant controls on the local hydrogeology: the Columbia River fault and the Slocan Lake fault. Both have previously been interpreted as low-angle, east-dipping, brittle normal faults, with a range of possible displacement. In the footwall (west side) of the Columbia River and Slocan Lake faults there are amphibolite- to granulite-grade metamorphic complexes, the Monashee and Valhalla, respectively. These, like the Malton gneiss complex near Valemount, are interpreted to be fragments of exhumed cratonic basement (Ross, 1991). Rocks in the hangingwalls are generally greenschist-grade metasedimentary rocks, and unmetamorphosed Jurassic and Cretaceous plutonic suites.

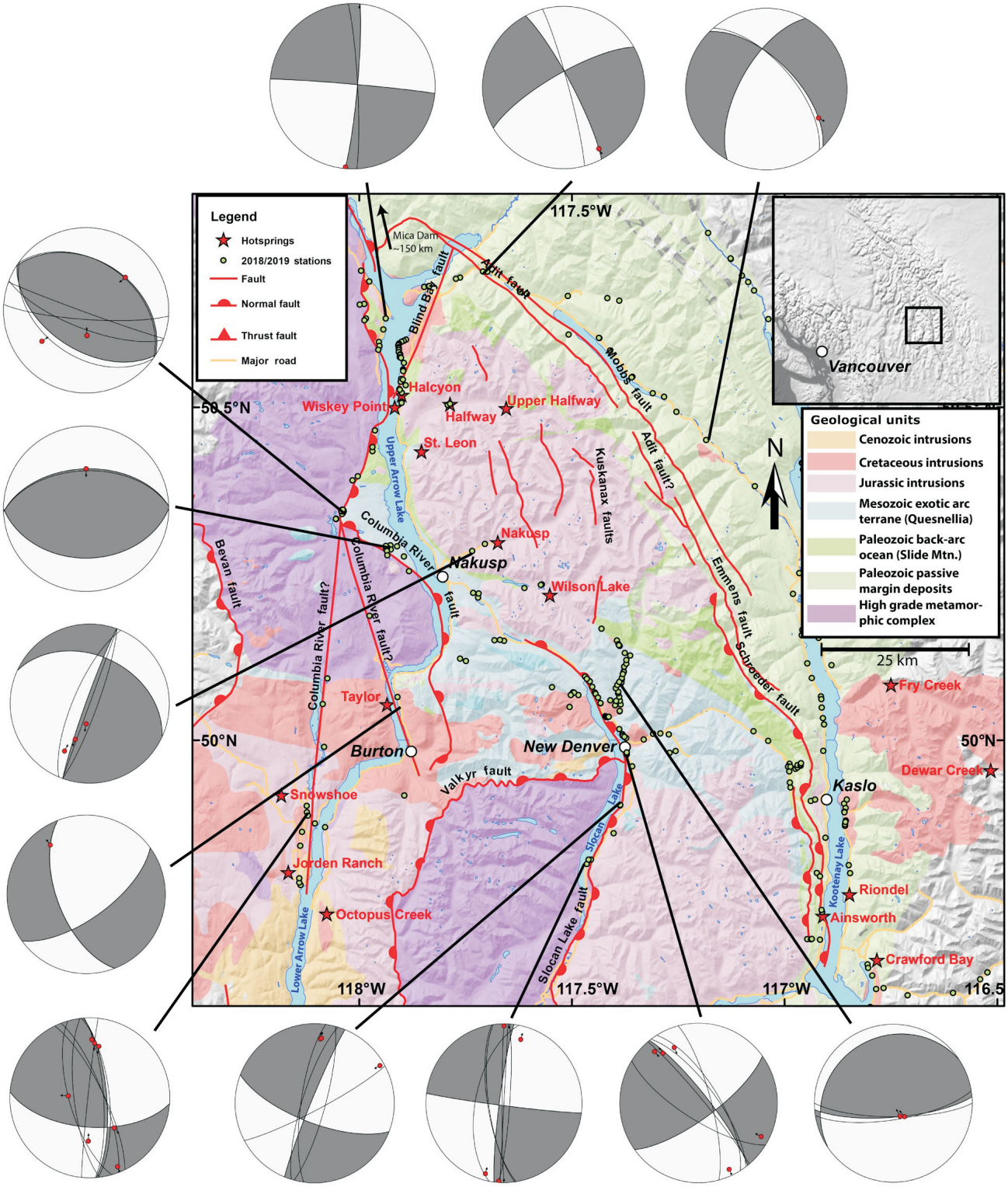


**Figure 4.** Geology of the West Kootenay region around Nakusp, British Columbia, after Cui et al. (2017). Lower-hemisphere stereonets show fault plane and slickenline orientations for subsets of stations. Compressional (P) and dilational (T) quadrants represent the average kinematics for each subset. Dextral kinematics were observed on the Columbia River fault and Slocan Lake fault, whereas reverse kinematics were observed in the transfer zone between Nakusp and New Denver.

The Columbia River fault (CRF) extends ~225 km southward from the Mica hydroelectric dam (52°N) to the hamlet of Burton on Lower Arrow Lake (50°N). At its northern end, it merges with the RMT fault in Kinbasket Lake (Figure 1b). At its southern end, mapped displacement across the fault gradually wanes to zero. Dip-slip displacements estimated on the basis of offset metamorphic isograds range from <1 km (Lemieux et al., 2003), 1–10 km (Lane, 1984), 15–80 km (Read and Brown, 1981) and 30 km (Parrish et al., 1988). Excavations during construction of the Revelstoke hydroelectric dam in the late 1970s provided the opportunity for detailed structural analysis of the brittle Columbia River fault. Lane (1984) measured the orientation of kinematic indicators at the damsite and at several sites along Highway 23 to the north of the dam. He concluded that primary displacement was extensional dip-slip, with a later phase of dextral strike-slip motion that was deemed insignificant. He also concluded that the right-hand step in the trace of the fault at the damsite might be associated with vertical axis rotation during dextral transpression. South of Revelstoke, the fault is parallel to Upper Arrow Lake, and a segment is exposed onshore on the east side of the lake immediately south of the Galena Bay ferry terminal. Near Halcyon Hot Spring, the fault swings southwest across the lake, and then trends parallel to the west side of Saddle Mountain before terminating at the hamlet of Burton (Figure 4).

The Slocan Lake–Champion Lakes fault system extends ~140 km from Summit Lake along Highway 6 between Nakusp and New Denver, south along Slocan Lake, through Castlegar, ending near Montrose. Interpreted deep seismic reflection profiles from the Lithoprobe project indicate that the fault zone dips shallowly east, penetrating the Moho (Cook et al., 1992). The Slocan Lake fault (SLF) is coincident with and overprints the surface trace of a broad zone of ductile deformation, the Valkyr shear zone, that arches over the Valhalla metamorphic complex to the east (Carr et al., 1987). South of Castlegar, the SLF becomes known as the Champion Lakes fault, and is mapped as a moderate to steeply (40–80°) east-dipping normal fault with a minimum of 1–2 km of offset (Corbett and Simony, 1984).

## New Observations

Exposures of the brittle CRF and SLF described by previous authors were revisited in 2018 and 2019. At the Revelstoke damsite, both normal dip-slip and dextral strike-slip kinematic indicators were observed in a splay of the CRF, an observation consistent with that of Lane (1984). Farther south along the CRF, west of Nakusp, across Upper Arrow Lake, an outcrop of fault gouge originally interpreted as an exposure of the locally northwestward-striking CRF by Lemieux et al. (2003) was visited. The main schistose fabric of the footwall rock was observed to strike west, and is folded, forming small-amplitude south-vergent folds. Such deformation is consistent with reverse faulting during north-south shortening, rather than east-west extension. A similar reinterpretation was made at a nearby outcrop originally mapped by Thompson et al. (2004).

In the region between southern Upper Arrow Lake and northern Slocan Lake, a belt of east-west-trending faults and folds occurs at a high angle to the regional strike. Cretaceous and Cenozoic intrusions appear to be affected by this deformation: brittle faults are observed on the margins of plutons, and felsic sills that intruded along the primary cleavage planes are folded, forming south-verging folds (Figure 5b). Age constraints on these intrusions are sparse, so it is difficult to confirm the timing of this deformation, but it is at least post-Cretaceous, if not post-Eocene. This suggests that this region between the northern tip of the Slocan Lake fault and the southern tip of the Columbia River fault could be a restraining bend in a dextral system.

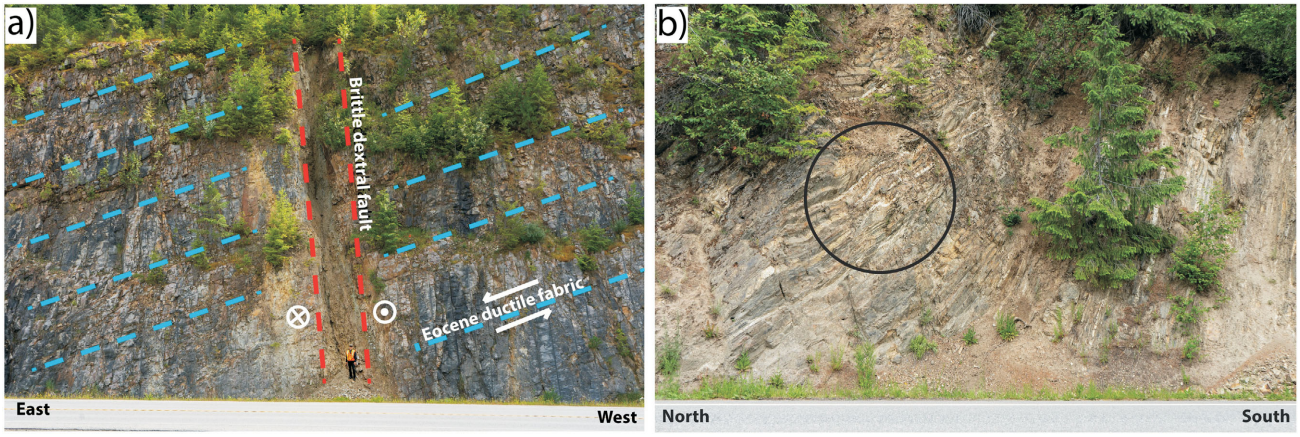


**Figure 5. a)** View south at outcrop on Highway 6 south of New Denver (lat. 49.8189°N, long. 117.4549°W). A 2 m wide subvertical brittle dextral fault oriented 172°/74° cuts across shallowly east-dipping (008°/31°) ductile fabric of the Slocan Lake fault/Valkyr shear zone. White encircled dot and "x" indicate motion towards and away from the viewer, respectively. **b)** View east at outcrop on Highway 6 north of New Denver (lat. 50.0555°N, long. 117.4323°W). Small, 20 cm wavelength, south-vergent folds are observed in felsic sills intruded parallel to the $S_1$ cleavage (oriented 278°/51°) of the Slocan phyllite. Circle is approximately 1.5 m wide.

At two locations along the east side of Slocan Lake, where the SLF crosses Highway 6, subhorizontal dextral slickenlines were observed on subvertical fault planes, in one case on a brittle fault that cuts through the Eocene-aged Ladybird granite (Carr, 1992), and on another that cuts at a high angle (Figure 5a) across the Eocene-aged ductile fabric of the Valkyr shear zone (Carr et al., 1987).

The Jurassic Kuskanax batholith, from which several thermal springs issue, has several north-south-striking faults mapped through its core, which appear to be subvertical based on their linear intersection with topography (Figure 4). Thompson et al. (2009) mapped these faults as dextrally offsetting roof pendants of Paleozoic metavolcanic rocks. It seems likely that these faults arose from the same transpression that caused dextral motion on the CRF.

## The Southern Rocky Mountain Trench and the Redwall Fault

### Background

There are seven thermal springs that occur along the eastern edge the southern Rocky Mountain Trench between the towns of Golden and Cranbrook (Figure 1b). Although the springs along the SRMT are not extremely hot, neither at depth nor at the surface (Grasby and Hutcheon, 2001), their close association with the Redwall fault (Figure 6) make them an interesting case study in structural controls of thermal springs in the Cordillera.

The Redwall fault is an enigmatic structure that has not been investigated in great detail since it was first mapped by Henderson (1954). Its surface trace extends from the hamlet of Edgeworth in the southern Rocky Mountain Trench, passing just east of Radium Hot Springs. It continues south along the Stanford Range, intersecting the Kootenay River at the Red Rock warm springs, before disappearing near Premier Lake. It has been suggested that it merges with the Lussier River fault to the south, which also hosts several thermal springs (Foo, 1979). The fault is subvertical for its entire length, leading several authors to conclude that it hosted either sinistral (Henderson, 1954) or dextral (Charlesworth, 1959) motion. More recently, Foo (1979) considered the Redwall fault to be a back-rotated thrust fault.

The Redwall Fault is so-named due to the striking red colour of the fault zone, caused by hematite oxidation (Figure 7b). The fault zone occurs in conjunction with a zone of subangular to subrounded, matrix-supported pebble to boulder conglomerate. This texture was originally interpreted to represent a zone of Cretaceous fault breccia (Henderson, 1954), but subsequent investigations have suggested that most of the breccia may be due to pre-Cretaceous evaporite-solution collapse (Stanton, 1966; Price, 2000), a theory supported by the proximity of extensive gypsum deposits (Henderson, 1954). Stratigraphic offsets, and evidence of shearing within the conglomerate, indicate that it has subsequently been reworked by faulting (of uncertain kinematics), following a décollement in the evaporites.

### New Observations

Exposures of the Redwall fault near Radium, Invermere and Canal Flats were visited in 2019. Dextral kinematic indicators were observed at exposures of the fault immediately east of Radium Hot Springs, along the Westroc mine road east of Invermere, and at the Red Rock warm springs on the Kootenay River forest service road (Figures 6, 7). An outcrop on a forest service road southwest of Lussier Hot Springs displays red- and orange-stained microbreccia and abundant slickenlines. It appears to share similar characteristics with the Redwall fault, suggesting the Redwall fault does not continue into the Lussier River fault as previously suggested, but instead re-merges with the Rocky Mountain Trench fault to the south-southwest (Figure 6). Dextral kinematics were also observed near the south end of the Lussier River fault, on a small splay fault, indicating that dextral shear is distributed throughout the area.

It seems likely that the combination of primary permeability of the conglomerate, and secondary permeability of fractures, is what makes this single structure such a great host of thermal springs. It is clear from the oxidation of conglomerate clasts and surrounding matrix material, that the Redwall fault has a protracted history of hydrothermal flow. For example, at Red Rock warm springs, a large, layered tufa dome is present at the top of the cliff on the north side of the Kootenay River. The dome is bisected by the cliff such that the interior is visible, and no thermal water presently flows. Another tufa deposit occurs a few kilometres to the east along the forestry road. It is evident that hydrothermal flow on the Redwall fault is ephemeral, and that thermal springs have migrated along it through time.

# Discussion

## Fault Kinematics, Regional Stress and Fault Permeability

New field observations and structural measurements from this study have revealed three significant insights into the structural characteristics governing fluid flow on fault zones in the southeastern Canadian Cordillera: 1) the most recent brittle fabric developed in these fault zones includes subvertical, rather than shallowly dipping, shear surfaces; 2) dominant fault kinematics are dextral, and perhaps reflect a reactivation of older extensional structures; and 3) crosscutting relationships show that at least some of these faults were active after the Eocene. These insights are important for understanding where local zones of active

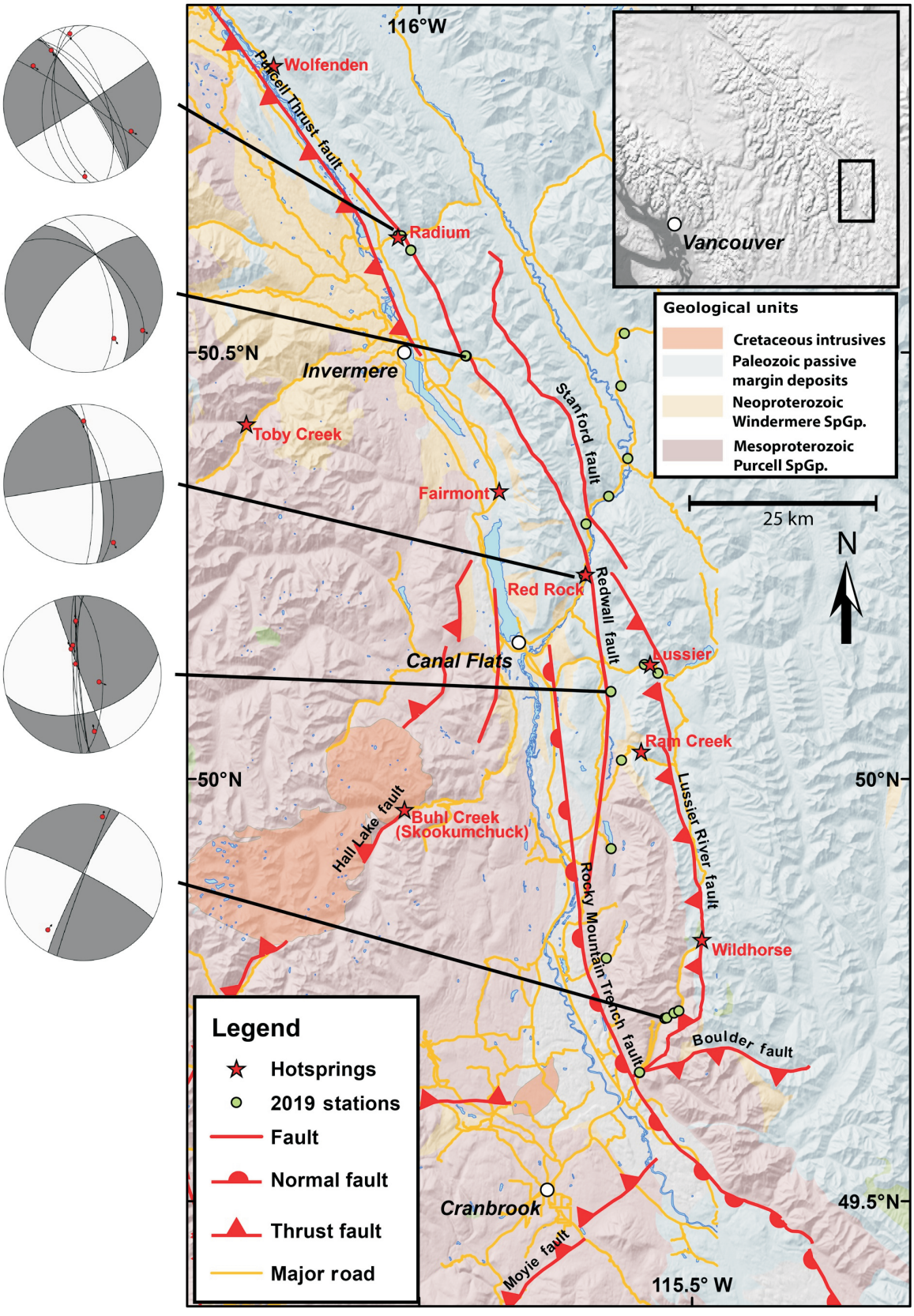


**Figure 6.** Geology of the southern Rocky Mountain Trench from Radium to Cranbrook, after Cui et al. (2017). Lower-hemisphere stereonets show fault plane and slickenline orientations for subsets of stations. Compressional (P) and dilational (T) quadrants represent the average kinematics for each subset. Dextral fault kinematics were observed on the Redwall fault at several locations. Abbreviation: SpGp., Supergroup.


**Figure 7. a)** Looking southwest at a tufa dome atop a cliff at the Red Rock warm springs on the Kootenay River (lat. 50.2389°N, long. 115.6963°W). No thermal water currently issues from the tufa dome. **b)** View south of the Redwall fault zone from Redstreak Mountain (lat. 50.6149°N, long. 116.0242°W). **c)** Looking east at a dextral fault plane oriented 304°/86° within the Redwall fault zone near Radium Hot Springs. Red arrow shows slickenline orientation (30°→119°).

slip, dilation and extension might facilitate the upward flow of thermal water.

In amagmatic, structurally controlled geothermal systems, the orientation of the current regional stress field relative to crustal faults is a critical factor in characterizing fault permeability. Faults and fractures that are oriented parallel to, or between 30° and 45° to the stress field, will either dilate or slip, respectively, thus permitting the flow of fluid (Sibson, 1994; Barton et al., 1995). Furthermore, it has been shown that local regions of extension (e.g., releasing bends), especially in active transpressional systems, are particularly favourable for fluid flow (Curewitz and Karson, 1997; Faulds and Hinz, 2015).

The current stress state of the crust within the Cordillera is not well constrained. The measurements that do exist are derived from the inversion of moment tensors for earthquakes of moment magnitude ($M_w$) 4 and greater (Ristau et al., 2007). Southeastern BC has a low level of seismic activity compared to the active margin on the west coast, and only four earthquakes of $M_w$ 4 or greater have occurred since record-keeping began in 1976. However, it is noteworthy that all these earthquakes have focal mechanisms that are consistent with dextral strike-slip motion on roughly north-south-striking fault planes due to a north-northeast–south-southwest oriented $S_{Hmax}$ (Ristau et al., 2007).

The alignment of the current $S_{Hmax}$ vectors with the T-axes of 'beachball' plots derived from field measurements further suggests that the crustal earthquakes and observed fault kinematics are both manifestations of neotectonic strain in the Cordillera. In other words, it is possible that these faults are still active at a low level due to the current stress field. Thus, a rudimentary analysis of slip and dilation tendency (e.g., Meixner et al., 2018) can be performed, in order to determine which faults may be most permeable under the present stress field. Maximum dilation will occur on faults and fractures oriented parallel to $S_{Hmax}$, whereas maximum slip will occur on segments oriented 30–45° oblique to $S_{Hmax}$ (Figure 8). Faults oriented perpendicular to $S_{Hmax}$ will likely be less permeable. In Figure 8, the average orientation of the SLF, CRF, PTrF and RMTF are plot-

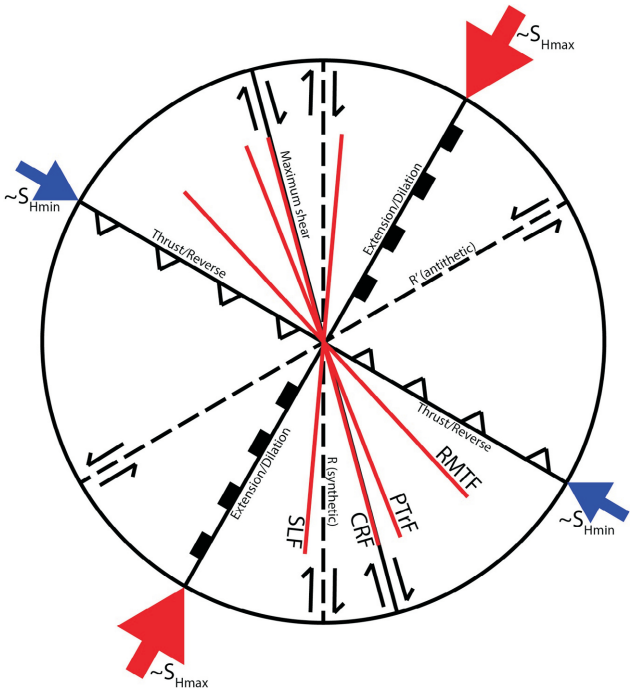


**Figure 8.** Strain ellipse for approximate $S_{Hmax}$ (maximum horizontal compression) orientation in southeastern British Columbia (Ristau et al., 2007), and corresponding predicted modes of brittle deformation on faults and fractures. Average orientations of the Rocky Mountain Trench fault (RMTF), Purcell Trench fault (PTrF), Columbia River fault (CRF) and Slocan Lake fault (SLF) are shown for reference.

ted relative to the approximate $S_{Hmax}$ orientation in the southeastern Cordillera (Ristau et al., 2007). In this configuration, the CRF, SLF and PTrF are oriented favourably for dextral slip, whereas the RMTF might experience more transpression. However, this simplistic representation of the regional strain does not capture local variability in fault geometry and stress orientations.

## The Possibility of Blind Geothermal Systems

Convective geothermal systems with no modern surface manifestation (called blind systems) are known to occur in active geothermal fields throughout the world. For example, blind systems constitute nearly 40% of known systems in Nevada, and it is likely that far more are yet to be discovered (Faulds and Hinz, 2015). Conceptual models for these inconspicuous geothermal resources vary, but typically an impermeable layer blocks the ascent of fluids, or cold influx of shallow groundwater may dilute or divert a rising plume (Dobson, 2016). It is conceivable that similar blind systems exist in the Canadian Cordillera, masked by high infiltration rates of cold meteoric water. Precipitation rates are much higher in the Canadian Cordillera than in the arid Great Basin of the southwestern United States, and thick glaciogenic overburden may facilitate near-surface dispersion and dilution of any ascending plumes of geothermal brine. At least one blind geothermal system has been identified in the Canadian Cordillera, in the Bluebell mine at Riondel (Figure 4). During mine operation in 1956, workers encountered water approximately 20–30°C flowing from cracks at 90–1000 L/s at a depth of ~300 m below ground (Desrochers, 1992). This thermal water did not flow to the surface, or, if it did, it had already cooled below detectable levels. It is a statistical likelihood that other blind systems remain undiscovered elsewhere in the Canadian Cordillera, particularly due to the low "degree-of-exploration" (Coolbaugh et al., 2006) in the area. A first-order prediction of their location may come from identifying where local zones of slip and dilation occur, given the orientation of faults in the current crustal stress field.

## Conclusions

Potential geothermal resources in southeastern British Columbia (BC) are likely amagmatic and rely on the deep circulation of thermal fluid along permeable fracture pathways. This regional-scale investigation of the structural settings of hydrothermal systems in southeastern BC has revealed a consistent pattern of dextral kinematics on brittle subvertical fault planes coincident with the surface traces of faults previously mapped as Eocene and Jura-Cretaceous in age; dextral kinematic indicators characterize the Rocky Mountain Trench fault near Valemount, the Redwall fault near Invermere, the Columbia River fault near Nakusp, and the Slocan Lake fault near New Denver. The timing of this transpressional deformation is constrained to post-Eocene, based on crosscutting relationships observed in Eocene-aged rocks. The north-northeast–south-southwest stress field required for these kinematics is consistent with the focal mechanisms of several crustal earthquakes that have occurred in the region, suggesting that transpressional strain has persisted from the Eocene to recent. Faults oriented at 30–45° to $S_{Hmax}$ (maximum horizontal compression) are most likely to slip, thereby maintaining fault permeability. Likewise, fractures oriented parallel to $S_{Hmax}$ are most likely to dilate and allow for fluid flow. Future geothermal exploration efforts in southeastern BC should focus on fault segments oriented favourably in the stress field, especially in light of the possibility of blind geothermal systems.

## Acknowledgments

This research was conducted as part of the University of Alberta's Future Energy Systems project: Imaging, Characterizing and Modelling Canada's Geothermal Resources, a research initiative funded by the Canada First Research Excellence Fund. Additional support came from a Canada Graduate Scholarships-Masters Program award from the Natural Sciences and Engineering Research Council and a Hugh C. Morris Fellowship.

N. Van Camp, S. Johnson, J. Beales, N. Lee and K. Purdon are thanked for their efforts as field assistants. M. Hesketh is thanked for his help configuring the digital mapping software for tablet computers used in the field.

## References


Agemar, T., Weber, J. and Schulz, R. (2014): Deep geothermal energy production in Germany; Energies, v. 7, p. 4397–4416, URL <https://doi.org/10.3390/en7074397> [November 2019].

Allen, D.M., Grasby, S.E. and Voormeij, D.A. (2006): Determining the circulation depth of thermal springs in the southern Rocky Mountain Trench, south-eastern British Columbia, Canada using geothermometry and borehole temperature logs; Hydrogeology Journal, v. 14, p. 159–172, URL <https://doi.org/10.1007/s10040-004-0428-z> [November 2019].

American Geological Institute (2003): Global GIS: volcanoes of the world; American Geological Institute, URL <https://earthworks.stanford.edu/catalog/harvard-glb-volc> [July 2019].

Armstrong, R.L. (1988): Mesozoic and early Cenozoic magmatic evolution of the Canadian Cordillera; *in* Processes in Continental Lithospheric Deformation, S.P. Clark, Jr., B.C. Birchfiel and J. Suppe (ed.), Geological Society of America Special Papers, v. 218, p. 55–92, URL <https://pubs.geoscienceworld.org/books/book/356/chapter/3796583/Mesozoic-and-early-Cenozoic-magmatic-evolution-of> [November 2019].

Barton, C.A., Zoback, M.D. and Moos, D. (1995): Fluid flow along potentially active faults in crystalline rock; Geology, v. 23, p. 683–686, URL <https://doi.org/10.1130/0091-7613(1995)023<0683:FFAPAF>2.3.CO;2>[November 2019].

Blackwell, D. and Richards, M. (2004): Geothermal map of North America; American Association of Petroleum Geologists, Product Code 423, scale 1:6 500 000.

Caine, J.S., Evans, J.P. and Forster, C.B. (1996): Fault zone architecture and permeability structure; Geology, v. 24, p. 1025–1028, URL <https://pubs.geoscienceworld.org/gsa/geology/article-abstract/24/11/1025/187969/Fault-zone-architecture-and-permeability-structure?redirectedFrom=fulltext> [November 2019].

Caron, M., Grasby, S.E. and Ryan, M.C. (2007): Spring geochemistry: a tool for mineral exploration in the south Nahanni River basin of the Mackenzie Mountains, Northwest Territories; *in* Mineral and Energy Resource Assessment of the Greater Nahanni Ecosystem Under Consideration for the Expansion of the Nahanni National Park Reserve, Northwest Territories, D.F. Wright, D. Lemkow and J.R. Harris (ed.), Geological Survey of Canada, Open File 5344, p. 31–74.

Carr, S.D. (1992): Tectonic setting and U-Pb geochronology of the Early Tertiary Ladybird Leucogranite Suite, Thor–Odin–Pinnacles area, southern Omineca Belt, British Columbia; Tectonics, v. 11, p. 258–278, URL <https://doi.org/10.1029/91TC01644> [November 2019].

Carr, S.D., Parrish, R.R. and Brown, R.L. (1987): Eocene structural development of the Valhalla Complex, southeastern British Columbia; Tectonics, v. 6, p. 175–196, URL <https://doi.org/10.1029/TC006i002p00175> [November 2019].

Chamberlain, V.E. and Lambert, R.St.J. (1985): Cordilleria, a newly defined Canadian microcontinent; Nature, v. 314, p. 707–713, URL <https://www.nature.com/articles/314707a0> [November 2019].

Chamberlain, V.E., Lambert, R.St.J. and Holland, J.G. (1985): Geochemistry and geochronology of the gneisses east of the southern Rocky Mountain Trench, near Valemount, British Columbia; Canadian Journal of Earth Sciences, v. 22, p. 980–991, URL <https://doi.org/10.1139/e85-103> [November 2019].

Charlesworth, H.A.K. (1959): Some suggestions on the structural development of the Rocky Mountains of Canada; Journal of the Alberta Society of Petroleum Geologists, v. 7, no. 11, p. 249–256.

Colpron, M. and Nelson, J. (2011): A digital atlas of terranes for the northern Cordillera; Yukon Geological Survey, URL <http://www.geology.gov.yk.ca/> [July 2019].

Cook, F.A., Varsek, J.L., Clowes, R.M., Kanasewich, E.R., Spencer, C.S., Parrish, R.R., Brown, R.L., Carr, S.D. and Johnson, B.J. (1992): LITHOPROBE crustal reflection cross section of the southern Canadian Cordillera, 1, Foreland thrust and fold belt to Fraser River Fault; Tectonics, v. 11, p. 12–35.

Coolbaugh, M.F., Raines, G.L., Zehner, R.S.E., Shevenell, L. and Williams, C.F. (2006): Prediction and discovery of new geothermal resources in the Great Basin: multiple evidence of a large undiscovered resource base; GRC Transactions, v. 30, p. 867–873.

Corbett, C.R. and Simony, P.S. (1984): The Champion Lake Fault in the Trail-Castlegar area of southeastern British Columbia; *in* Current Research, Part A, Geological Survey of Canada, Paper 84-1A, p. 103–104.

Cui, Y., Miller, D., Schiarizza, P. and Diakow, L.J. (2017): British Columbia digital geology; BC Ministry of Energy, Mines and Petroleum Resources, BC Geological Survey, Open File 2017-8, 9 p., URL <https://www2.gov.bc.ca/gov/content/industry/mineral-exploration-mining/british-columbia-geological-survey/geology/bcdigitalgeology> [July 2019].

Curewitz, D. and Karson, J.A. (1997): Structural settings of hydrothermal outflow: fracture permeability maintained by fault propagation and interaction; Journal of Volcanology and Geothermal Research, v. 79, p. 149–168, URL <https://doi.org/10.1016/S0377-0273(97)00027-9> [November 2019].

Davis, E.E. and Lewis, T.J. (1984): Heat flow in a back-arc environment: Intermontane and Omineca crystalline belts, southern Canadian Cordillera; Canadian Journal of Earth Sciences, v. 21, p. 715–726.

Desrochers, D.T. (1992): Geothermal feasibility study for the use of hot water near Riondel, British Columbia; Geological Survey of Canada, Open File 2502, 108 p.

Dobson, P.F. (2016): A review of exploration methods for discovering hidden geothermal systems; GRC Transactions, v. 40, p. 695–706.

Evenchick, C., McMechan, M.E., McNicoll, V.J. and Carr, S.D. (2007): A synthesis of the Jurassic–Cretaceous tectonic evolution of the central and southeastern Canadian Cordillera: Exploring links across the orogen; *in* Geological Society of America, Special Paper 433, p. 117–145.

Farquharson, N., Schubert, A. and Steiner, U. (2016): Geothermal energy in Munich (and beyond): a geothermal city case study; GRC Transactions, v. 40, p. 189–196.

Faulds, J.E. and Hinz, N.H. (2015): Favorable tectonic and structural settings of geothermal systems in the Great Basin Region, western USA: proxies for discovering blind geothermal systems; *in* Proceedings World Geothermal Congress 2015, April 19–25, 2015, Melbourne, Australia, p. 1–6.

Ferguson, G. and Grasby, S.E. (2011): Thermal springs and heat flow in North America; Geofluids, v. 11, p. 294–301, URL <https://doi.org/10.1111/j.1468-8123.2011.00339.x> [November 2019].

Foo, W.K. (1979): Evolution of transverse structures linking the Purcell Anticlinorium to the western Rocky Mountains near Canal Flats, British Columbia; M.Sc. thesis, Queen's University.

Gabrielse, H. (1985): Major dextral transcurrent displacements along the Northern Rocky Mountain Trench and related lineaments in north-central British Columbia; Geological Society of America Bulletin, v. 96, p. 1–14, URL <https://doi.org/10.1130/0016-7606(1985)96<1:MDTDAT>2.0.CO;2>[November 2019].

Gabrielse, H. and Yorath, C.J. (1991): Tectonic synthesis; Chapter 18 *in* Geology of the Cordilleran Orogen in Canada, H. Gabrielse and C.J. Yorath (ed.), Geological Survey of Canada, Geology of Canada, no. 4, p. 677–705 (also Geological Society of America, Geology of North America, v. G-2).

Gabrielse, H., Monger, J.W.H., Wheeler, J.O. and Yorath, C.J. (1991): Part A: morphogeological belts, tectonic assemblages and terranes; Chapter 2 *in* Geology of the Cordilleran Orogen in Canada, H. Gabrielse and C.J. Yorath (ed.), Geological Survey of Canada, Geology of Canada, no. 4, p. 15–28.

Ghomshei, M.M. (2007): Qualifying report on: a high-grade geothermal resource in the Canadian Rockies, Canoe Hot Springs, Valemount, British Columbia; internal company report prepared for Comstock Energy Inc.

Grasby, S.E. and Hutcheon, I. (2001): Controls on the distribution of thermal springs in the southern Canadian Cordillera; Canadian Journal of Earth Sciences, v. 38, p. 427–440, URL <https://www.researchgate.net/publication/249543830_Controls_on_the_distribution_of_thermal_springs_in_the_southern_Canadian_Cordillera> [November 2019].

Grasby, S., Allen, D.M., Bell, S., Chen, Z., Ferguson, G., Jessop, A., Kelman, M., Ko, M., Majorowicz, J., Moore, M., Raymond, J. and Therrien, R. (2012): Geothermal energy resource potential of Canada; Geological Survey of Canada, Open File 6914 (revised), 322 p., URL <http://publications.gc.ca/collections/collection_2013/rncan-nrcan/M183-2-6914-eng.pdf> [November 2019].

Green, N.L., Armstrong, R.L., Harakal, J.E., Souther, J.G. and Read, P.B. (1988): Eruptive history and K-Ar geochronology of the late Cenozoic Garibaldi volcanic belt, southwestern British Columbia; Geological Society of America Bulletin, v. 100, p. 563–579, URL <https://doi.org/10.1130/0016-7606(1988)100<0563:EHAKAG>2.3.CO;2> [November 2019].

Henderson, G.G.L. (1954): Geology of the Stanford Range of the Rocky Mountains; BC Ministry of Energy, Mines and Petroleum Resources, BC Geological Survey, Bulletin 35.

Hitchon, B. (1984): Geothermal gradients, hydrodynamics, and hydrocarbon occurrences, Alberta, Canada; American Association of Petroleum Geologists Bulletin, v. 68, p. 713–743.

Hyndman, R.D. and Lewis, T.J. (1995): Review: the thermal regime along the southern Canadian Cordillera Lithoprobe corridor; Canadian Journal of Earth Sciences, v. 32, p. 1611–1617, URL <https://doi.org/10.1139/e95-129> [November 2019].

Jessop, A.M., Ghomshei, M.M. and Drury, M.J. (1991): Geothermal energy in Canada; Geothermics, v. 20, p. 369–385.

Lane, L.S. (1984): Brittle deformation in the Columbia River fault zone near Revelstoke, southeastern British Columbia; Canadian Journal of Earth Sciences, v. 21, p. 584–598, URL <https://doi.org/10.1139/e84-063> [November 2019].

Lemieux, Y., Thompson, R.I. and Erdmer, P. (2003): Stratigraphy and structure of the Upper Arrow Lake area, southeastern British Columbia: new perspectives for the Columbia River Fault Zone; Geological Survey of Canada, Current Research 2003-A7, 11 p.

Lewis, T.J., Bentkowski, W.H. and Hyndman, R.D. (1992): Crustal temperatures near the Lithoprobe Southern Canadian Cordillera Transect; Canadian Journal of Earth Sciences, v. 29, p. 1197–1214, URL <https://doi.org/10.1139/e92-096> [November 2019].

Majorowicz, J. and Grasby, S.E. (2010): Heat flow, depth–temperature variations and stored thermal energy for enhanced geothermal systems in Canada; Journal of Geophysics and Engineering, v. 7, p. 232–241, URL <https://www.researchgate.net/publication/228077909_Heat_flow_depth-temperature_variations_and_stored_thermal_energy_for_enhanced_geothermal_systems_in_Canada> [November 2019].

McDonough, M.R. and Simony, P.S. (1988): Structural evolution of basement gneisses and Hadrynian cover, Bulldog Creek area, Rocky Mountains, British Columbia; Canadian Journal of Earth Sciences, v. 25, p. 1687–1702, URL <https://doi.org/10.1139/e88-159> [November 2019].

McDonough, M.R. and Simony, P.S. (1989): Valemount strain zone: a dextral oblique-slip thrust system linking the Rocky Mountain and Omineca belts of the southeastern Canadian Cordillera; Geology, v. 17, p. 237–240, URL <https://doi.org/10.1130/0091-7613(1989)017<0237:VSZADO>2.3.CO;2> [November 2019].

McMechan, M.E. (2000): Walker Creek fault zone, central Rocky Mountains, British Columbia-southern continuation of the Northern Rocky Mountain Trench fault zone; Canadian Journal of Earth Sciences, v. 37, p. 1259–1273, URL <https://doi.org/10.1139/e00-038> [November 2019].

Meixner, J., Grimmer, J.C., Becker, A., Schill, E. and Kohl, T. (2018): Comparison of different digital elevation models and satellite imagery for lineament analysis: implications for identification and spatial arrangement of fault zones in crystalline basement rocks of the southern Black Forest (Germany); Journal of Structural Geology, v. 108, p. 256–268, URL <https://doi.org/10.1016/j.jsg.2017.11.006> [November 2019].

Meixner, J., Schill, E., Grimmer, J.C., Gaucher, E., Kohl, T. and Klingler, P. (2016): Structural control of geothermal reservoirs in extensional tectonic settings: an example from the Upper Rhine Graben; Journal of Structural Geology, v. 82, p. 1–15, URL <https://doi.org/10.1016/j.jsg.2015.11.003> [November 2019].

Moeck, I.S. (2014): Catalog of geothermal play types based on geologic controls; Renewable and Sustainable Energy Reviews, v. 37, p. 867–882, URL <https://doi.org/10.1016/j.rser.2014.05.032> [November 2019].

Moreno, D., Lopez-Sanchez, J., Blessent, D. and Raymond, J. (2018): Fault characterization and heat-transfer modeling to the Northwest of Nevado del Ruiz Volcano; Journal of South American Earth Sciences, v. 88, p. 50–63, URL <https://doi.org/10.1016/j.jsames.2018.08.008> [November 2019].

Murphy, D.C. (1990): Direct evidence for dextral strike-slip displacement from mylonites in the southern Rocky Mountain Trench near Valemount, British Columbia; *in* Current Research, Part E, Geological Survey of Canada, Paper 90-1E, p. 91–96.

Murphy, D.C. (2007): Geology: Canoe River; Geological Survey of Canada, "A" Series Map 2110A, scale 1:250 000.

Parrish, R.R. and Wheeler, J.O. (1983): A U-Pb zircon age from the Kuskanax batholith, southeastern British Columbia; Canadian Journal of Earth Sciences, v. 20, p. 1751–1756, URL <https://doi.org/10.1139/e83-165> [November 2019].

Parrish, R.R., Carr, S.D. and Parkinson, D.L. (1988): Eocene extensional tectonics and geochronology of the Southern Omineca Belt, British Columbia and Washington; Tectonics, v. 7, p. 181–212, URL <https://doi.org/10.1029/TC007i002p00181> [November 2019].

Price, R.A. (1981): The Cordilleran foreland thrust and fold belt in the southern Canadian Rocky Mountains; Geological Society London, Special Publications, v. 9, p. 427–448, URL <https://www.researchgate.net/publication/249548179_The_Cordilleran_foreland_thrust_and_fold_belt_in_the_southern_Canadian_Rocky_Mountains> [November 2019].

Price, R.A. (2000): The southern Canadian Rockies: evolution of a foreland thrust and fold belt; GeoCanada Conference, May 29–June 2, 2000, Calgary, Alberta, Field Trip Guidebook, 244 p.

Price, R.A. and Carmichael, D.M. (1986): Geometric test for Late Cretaceous-Paleogene intracontinental transform faulting in the Canadian Cordillera; Geology, v. 14, p. 468–471, URL <https://doi.org/10.1130/0091-7613(1986)14<468:GTFLCI>2.0.CO;2> [November 2019].

Read, B. and Brown, R.L. (1981): Columbia River fault zone: southeastern margin of the Shuswap and Monashee complexes, southern British Columbia; Canadian Journal of Earth Sciences, v. 18, p. 1127–1145.

Reyes, A.G. (2015): Low-temperature geothermal reserves in New Zealand; Geothermics, v. 56, p. 138–161, URL <https://doi.org/10.1016/j.geothermics.2015.04.004> [November 2019].

Ristau, J., Rogers, G.C. and Cassidy, J.F. (2007): Stress in western Canada from regional moment tensor analysis; Canadian Journal of Earth Sciences, v. 44, p. 127–148, URL <https://doi.org/10.1139/e06-057> [November 2019].

Roddick, J.A. (1967): Tintina Trench; Journal of Geology, v. 75, p. 23–33.

Rogers, G.C., Ellis, R.M. and Hasegawa, H.S. (1980): The McNaughton Lake earthquake of May 14, 1978; Bulletin of the Seismological Society of America, v. 70, p. 1771–1786.

Ross, G.M. (1991): Precambrian basement in the Canadian Cordillera: an introduction; Canadian Journal of Earth Sciences, v. 28, p. 1133–1139, URL <https://doi.org/10.1139/e91-103> [November 2019].

Sibson, H. (1994): Crustal stress, faulting and fluid flow; *in* Geofluids: Origin, Migration, and Evolution of Fluids in Sedimentary Basins, Geological Society Special Publication 78, p. 69–84.

Stanton, R.J., Jr. (1966): The solution brecciation process; Geological Society of America Bulletin, v. 77, p. 843–848, URL <https://doi.org/10.1130/0016-7606(1966)77[843:TSBP]2.0.CO;2> [November 2019].

Struik, L.C. (1993): Intersecting intracontinental Tertiary transform fault systems in the North American Cordillera; Canadian Journal of Earth Sciences, v. 30, p. 1262–1274, URL <https://doi.org/10.1139/e93-108> [November 2019].

Thompson, R.I., Glombick, P. and Lemieux, Y. (2004): Geology: Mount Fosthall; Geological Survey of Canada, Open File 4377, scale 1:50 000.

Thompson, R.I., Lemieux, Y., Glombick, P. and Dhesi, P. (2009): Geology: St. Leon Creek; Geological Survey of Canada, Open File 6185, scale 1:50 000.

van der Velden, A.J. and Cook, F.A. (1996): Structure and tectonic development of the southern Rocky Mountain trench; Tectonics, v. 15, p. 517–544, URL <https://doi.org/10.1029/95TC03288> [November 2019].

Vollmer, F.W. (2019): Orient: spherical projection and orientation data analysis software user manual; Frederick W. Vollmer, URL <https://www.frederickvollmer.com/orient/download/Orient_User_Manual.pdf> [July 2019].

Woodsworth, G. and Woodsworth, D. (2014): Hot Springs of Western Canada: A Complete Guide, 3rd Edition; Gordon Soules Book Publishers, West Vancouver, British Columbia, 303 p.